



Uniaxial Tensile Simulation of 3D Orthogonal Woven Fabric

Yahya, M.F.^{1,*}, Ghani, S.A.¹ and Zahid, B.²

¹Textile Research Group, Faculty of Applied Sciences
Universiti Teknologi MARA, Shah Alam, Selangor, +60355444571

²Textile Engineering Department, NED University of Engineering & Technology,
University Road, Karachi, 75270, Pakistan

*Corresponding author e-mail: mfy@salam.uitm.edu.my

Abstract

Mesoscale modelling approach has shown close simulation approximations of woven fabric tensile performance. The main purpose of the work is to develop understanding of geometrical model development, finite element analysis procedure and to compare the differences of 2D and 3D woven fabric uniaxial tensile stress-strain. 3D woven fabric structures selected for the work is three-layer orthogonal woven fabrics. The woven structure will have 2 through-thickness warps, 4 non-crimps warp and 6 wefts. Through-thickness warp yarn will apply plain 1/1 weave structure for stitching all weft layers and non-crimps weft yarn together. Woven geometric models were developed with pre-processor program at detail yarn configurations. Simulation results showed that 3D orthogonal woven fabric had a better tensile response than its 2D woven fabric structures.

Keywords: *finite element analysis; orthogonal woven; three dimensional (3D); uniaxial tensile; weave unit cell*

1. Introduction

Complex woven textiles have many versatile characteristics that enabled them to infiltrate technical textiles application, particularly automotive, medical textile, sports and leisure. Engineers and scientists have realised that complex woven, particularly 3D fabrics, with reinforcement built into the longitudinal, transverse and thickness axes, offer strong, lightweight and mouldable material that can be manufactured with specific strength requirement using high performance fibres. 2D woven structure will provide in-plane stiffness, compression and strength in both warp and weft directions, but poor in interlaminar performance [1-3]. In addition to that, 2D laminated is difficult to be mould for complex shape. Higher manufacturing cost is also anticipated since 2D laminates need to be cut during fabrication process [1]. 3D fabric such as angle interlock and orthogonal weaves will provide stiffness not only in-plane direction, but also in through-thickness or in x-y-z directions [4]. The presence of through thickness reinforcement in z-direction also resulted in higher delamination resistance for 3D woven fabric [1], [5-8]. 3D woven fabric becomes serious candidates for impact resistance and energy absorbent composites [9-12].

3D woven fabric properties are highly correlated with crimp, non-crimp and through thickness yarn. Crimp is often associated with weave structure. The higher number of interlacing, then the higher number of crimps would be. Plain weave will have the highest number of crimps compared to twill and satin weave. Crimps presence in the woven fabric will allow greater non-linear rate on a tensile extensional curve. In view to this, Yang [2] reported that, crimp density in the orthogonal weave is mainly governed by vertical segment density of binder warp yarn and weft density, which determines the curve shape of load extension at low strain region.

Similarly, Whitcomb conducted research to understand the waviness or crimp effect to woven composites. The work developed a 3-dimensional model to evaluate the waviness properties of plain, twill and satin weaves. The work highlighted that waviness properties are also depended to weaves. It was reported that in-plane modulus E_1 is strongly responded to crimp change [13].

The non-crimp fabric is produced by minimizing interlacing sequence in the woven structure. The orthogonal fabric is an example of non-crimp fabric. In the structure, the fabric is bonded together when warp yarn performed stitching from top to bottom fabric layers. At the same time, additional "straight" yarns known as warp fillers and weft fillers are also introduced in the structure to increase fabric layers and thickness. Gu worked on tensile properties for various 3D woven fabric, had found that, yarn bending behaviour is a major factor when considering strength of the composites. Stronger composites are attributed to straight filament arrangement or reduce bending effect as much as possible [14]. Additionally, Adanur reported woven fabric modulus can be increased by reducing crimp in loading direction and crimp interchange in transverse direction with consideration of exploiting higher yarn modulus [15].

Many works reported that 3D woven fabric posse's high delamination resistance, due to the presence of through thickness yarn or sometimes referred to as z-binder [16-17]. Different fabric layers are bonded together, enhancing structural toughness and integrity during loading deformation cycle. The ability of 3D weaving to produce near net shape can greatly reduce the cost of the component by reducing material wastage, the need for machining and joining and the amount of material handled during lay-up. In terms of mouldability, 3D woven fabric can be moulded in several shapes to fit its new technical application. For the same reason, mouldability will prevent inherent cut and sew process, which would reduce strength due to destruction in fibre continuity. For example,

lightweight aircraft seat can be made from moulded 3D textile reinforcement to form specific shapes without wrinkles [18]. Another application is as military helmets, where a single piece of fabric is used as a precursor for protective reason. Chen highlights that, mouldability of angle-interlock fabrics is closely related to fabric density, shear rigidity and number of weft layers [19]. Additionally, most 3D structures fabrics can be produced using conventional dobby and jacquard looms. This allows immediate production and product availability with competitive product cost.

3D woven fabrics are also reported to have several properties drawbacks. One of the main drawbacks of 3D weaving is the inability of current looms to produce fabrics that contain in-plane yarn other than 0 and 90°. The fabric is considered too anisotropic. This in turn leads to poor shear and torsion performance.

2. Research Method

2.1. Yarn Modelling and Simulation

Yarn was assumed to have solid monofilament structure as compared to multi-filament in finite element simulation. Yarn structure was also treated to have uniform cross section throughout its length [8, 17, 22]. The primary task of the section was to develop lenticular shape yarn model, perform uniaxial yarn tensile analysis and compare with its respective experimental results. The yarn geometry was developed with ABAQUS CAE pre-processor tool with 3-points arch line tool in parts module. Yarn geometry model was developed according to yarn width; A at 1.29 mm and height, B at 0.35 mm. Yarn model stress magnitude was calculated at 3275 Nmm². Stress magnitude was determined by determining the ratio between 5000N uniaxial loads applied and its yarn cross sectional area of 0.31 mm². Uniaxial tensile simulation was performed by constraining one yarn edge while load was given on another opposite edge. The constrained rule or commonly referred to as boundary condition is a set of instructions given to models in finite element analysis to manage its response upon given load. In the simulation, yarn was allowed to move only in longitudinal direction, Z. This was simplified by the following Equation 1. The following (a) and (b) illustrate the load with boundary conditions and mesh selected for the model, respectively.

$$U_1 = U_2 = UR_1 = UR_2 = UR_3 = 0 \quad \text{Equation 1}$$

The yarn geometry had to be meshed to achieve efficient analysis time. For simulation stability, three dimensional (3D) yarn models were meshed with 11,667 elements and 19,182 nodes. The yarn geometry was meshed with 8 nodes hexahedron linear with reduced integration. The increase of elements numbers had resulted in excessive computing processing time. Finite element analysis was performed with yarn material property defined as isotropic elastic-plastic. Aramid yarn density was determined earlier from density test at 1.33 g cm⁻³. Poisson ratio was taken from literatures at 0.35 [4-5].

Simultaneous work was done to evaluate tensile properties of kevlar yarn. The data generated from the experimental work had not only served for experimental and simulation validation purpose but also provided information for yarn elastic modulus in simulation. Aramid yarn tensile strength was performed according to British Standard-ISO 2062 single yarn strength method [6]. The test requires specimen length at 250 mm with maximum load of 5000N and crosshead speed of 100 mm min⁻¹. Yarn tensile was performed on Instron tensile tester machine. Yarn modulus from experimental test was determined to be 15.88 MPa and adopted in isotropic property module in ABAQUS.

The use of experimental yarn modulus in ABAQUS material module had solely provided elastic behavior of woven fabric. In the analysis, yarn will continue to extend upon load and but even-

tually recover to original state once the load is released or removed. Additional procedure is needed to introduce plasticity behavior in both yarn and woven fabrics. For that reason, experimental yarn stress-strain curve had to be converted to account yarn plasticity behavior during uniaxial loading process. This was achieved by adopting Equations (2) and (3).

$$\varepsilon^p = \varepsilon^t - \varepsilon^e = \varepsilon^t - \frac{\sigma}{E} \quad \text{Equation 2}$$

$$\sigma = \sigma_{norm}(1 + \varepsilon_{norm}) \quad \text{Equation 3}$$

Where;

ε^{pl}	= true plastic strain	E	= modulus
ε^t	= true total strain	σ_{norm}	= nominal stress
ε^{el}	= true elastic strain	ε_{norm}	= nominal strain
σ	= true stress		

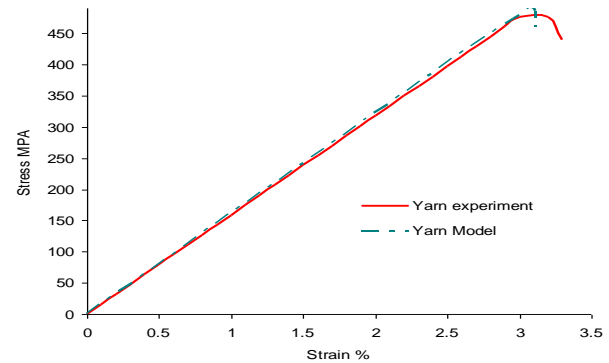


Figure 1.:Yarn tensile experiment and validation result

Figure 1 presents the stress-strain comparison analysis between yarn experimental and simulation results. The numerical comparison of experimental and simulation data are represented in the **Error! Reference source not found..** From the figure, the tensile results of both simulation and experimental uniaxial tensile results displayed linear stress-strain behavior until the yarn reached maximum peak of stress and strain points. The maximum stress and strain difference between simulations and experimental results were recorded at 2.9% and 1.3%, respectively. The modulus between experiment and simulation result were compared and reported variance of 0.7%. The results had shown close experimental and simulation validation were achieved with the appropriate yarn density, experimental yarn modulus and packing factor data.

	Simulation	Experiment
Max. stress (MPa)	490	476
Max. strain (%)	3.07	3.03
Modulus (MPa)	15989	15880

2.2. Yarn Linear Density Consideration

Another important issue to be considered is to incorporate yarn linear density effect in the model. Yarn linear density not only influenced fabric fineness or coarseness but also its mechanical properties such as tensile. An approach has been made to convert yarn linear density in Tex into fabric density in gm cm⁻³. An individual yarn mass (gm) can be determined by measuring yarn model lengths and using tex definition, i.e grams in 1000 meters. Later, yarn and fabric density are known by determining ratios between yarn mass (gm) and yarn volume (cm³). Fabric or yarn density should be the same at 1.44 g cm⁻³, regardless the dimension size. The calculated fabric density is 1.423 g cm⁻³, which is closed to yarn density adopted in the research.

2.3. Fabric Geometry Model Development

Warp, weft and non-crimp yarns geometrical models will have a lenticular cross section. Based on experimental stereomicroscope done during first year, yarn width and thickness are measured as 2.41 mm and 0.35 mm, respectively. With the value, yarn aspect ratio is calculated from yarn width and thickness to be 6.8. For computer aided design work in ABAQUS pre-processor, equivalent yarn aspect ratio is adopted for yarn geometrical model from 0.4 mm width and 0.0588 mm thickness.

2.4. Yarn Path

Yarn path geometry defined should able to accommodate yarn movement in the z-direction for packing all weft yarn layers. To design efficient warp yarn path movement in a through-thickness direction, twelve lenticular shape geometries are prepared to represent weft and non-crimp warp. Geometrical notation to represent yarn path is defined in the following equations 4 to 7.

$$\text{Structural length, } l = \frac{1}{2} p + w + p + w + \frac{1}{2} p = 1.5 p + 2w \quad \text{Equation 4}$$

$$\text{Yarn spacing, } p = t \quad \text{Equation 5}$$

$$\text{Through thickness yarn path, } z = 5t \quad \text{Equation 6}$$

$$\text{Bending zone, } c = -0.5587x^2 + 0.0294 \quad \text{Equation 7}$$

Yarn bending in zone c is calculated from a polynomial function $ax^2 + bx + c = y$ of lenticular shape derived of three distinct coordinates, namely (0.0294,0), (-0.2294,0) and (0, 0.2294). By plugging $x=0$ and $y=0.0294$ in the polynomial function, the value of c can be determined. Later, a and b values can be found by simultaneously solving two polynomial equations of two remaining sets of coordinates. However, for both non-crimp warp and weft yarn, the value of c and z is zero, since no interlacing effect is considered. Since both of these yarns are straight, yarn path equation is simplified according to the following equation 8 and 9. The following Figure 2 and Figure 3 described non-crimp warp and weft yarn paths. The figures also highlighted the W_{nc} , w, p and W_f notations in detail.

$$\text{Non-crimp warp path, } W_{nc} = 2w + p \quad \text{Equation 8}$$

$$\text{Weft path length, } W_f = 4w \quad \text{Equation 9}$$

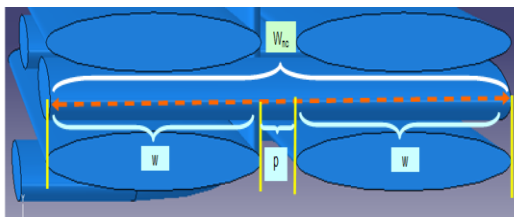


Figure 2: Non-crimp warp path

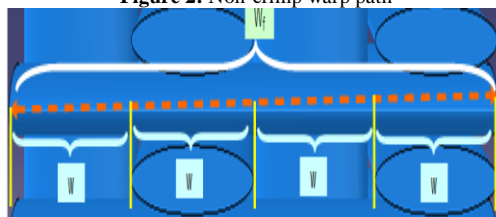


Figure 3: Weft yarn path

2.5. Load, Boundary Conditions and Mesh

Through thickness and non-crimp warp are assigned with “encastre” type boundary condition at boundary condition zone. Warp yarns are restrained to move in lengthwise or rotational wise. At the same time, uniaxial force is applied in loading zone at 844 MPa per yarn. The force is based on 5000 N load imposed during tension test on 6 warp yarns. The approach is necessary to establish uniaxial yarn tension effect for analysis. Figure 4 outlines boundary condition and the load applied in 3D orthogonal woven fabric. Yarn interactions in 3D orthogonal woven fabric are defined to have an explicit general contact at 0.2 coefficients. This method will acknowledge yarn mobility in the 3D structure and not completely fused as in the case of 2D woven fabrics. Many literatures have indicated 3D woven fabrics to have lower shear due to the presence of through thickness yarn [22], [23]. Tetrahedron element has been selected for meshing yarns prior to finite element analysis to commence. Tetrahedron element is adopted as it allows mesh formation for nonlinear geometrical set-up. Total elements established from the procedure are 46,456. More elements are seeded in weft yarn because of additional length it has compared to through-thickness warp and non-crimp warp. The following Figure 5 illustrates 3D orthogonal woven fabric after meshing procedure and Table 2 presented mesh for each component in the model.

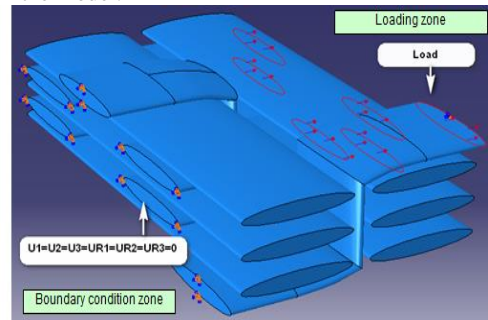


Figure 4: Loading and boundary condition

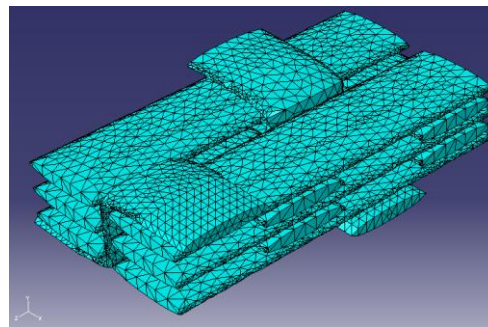


Figure 5: Mesh

Table 2: Mesh breakdown

	Mesh per yarn	Number of yarns	Total mesh
Through thickness warp	4165	2	8330
Non-crimp warp	2417	4	9668
Weft	4743	6	28458
Total mesh			46456

3. Stress-Strain Results

Simulation results of 3D orthogonal woven fabric model and 2D woven fabric is presented together for comparison in Figure 6. It is very clear that 3D orthogonal woven fabric showed superior stress-strain performance compared to plain (PW), twill (TW) and satin (SW) woven fabric models. 3D orthogonal woven fabric reported highest 76 MPa stress, which is twice than SW at 2.2% strain. Within equivalent strain, PW the reported lowest stress at 16 MPa, followed by TW at 25 MPa and SW at 38 MPa. Additionally, 3D woven fabric has continued to report stress increment

beyond 3% strain, while all 2D woven fabrics have started to yield constant or declining stress. Non-crimp yarn presence in 3D woven fabric has drastically improved its uniaxial tensile behavior. Less crimp in woven fabric structure would assist in further load bearing capacity, leading to higher stress-strain results. This is consistent with finding made by other researchers [3,24,25]. The presence of non-crimp yarn in 3D woven fabric would promote higher and linear stress-strain curve as compared to the non-linear behavior of 2D woven fabric models. This finding is in tandem with following Figure 6 that presented higher stress concentration to occur more in non-crimp yarn compared to through-thickness warp yarn.

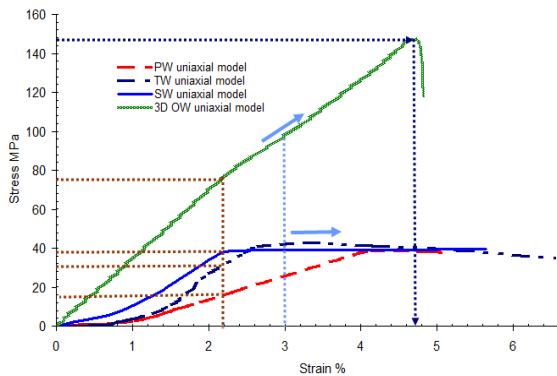


Figure 6: Stress-strain analysis

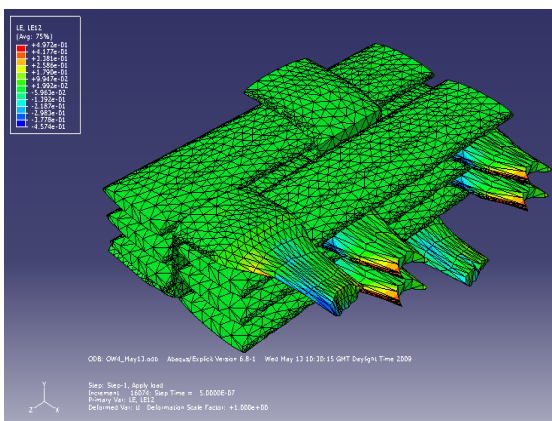


Figure 7: Stress concentration areas

4. Conclusions

Experimental and finite element analysis of yarn and woven fabrics for uniaxial tensile of 3D orthogonal woven fabrics were reviewed and validated, by using isotropic elastic-plastic material properties. Non-crimp yarn in 3D orthogonal woven fabric would assist higher uniaxial tensile performance. The non-crimp yarn has fewer built-in stresses as compared to its respective crimp yarns, and responded immediately to uniaxial tensile. The finding is consistent with yarn and satin woven fabric uniaxial tensile test. The simulation allowed stress distribution during uniaxial tensile and allow better selection of load bearing yarn for use.

References

- [1] Mouritz AP, Bannister MK, Falzon PJ, Leong KH (1999), Review of Applications for Advanced Three-Dimensional Fibre Textile Composites. *Compos Part A Appl Sci Manuf.* 30, 1445–61.
- [2] Yang C, Kim YK, Qidwai UA, Wilson AR (2004), Related Strength Properties of 3D Fabric. *Text Res J.* 74(7), 634–9.
- [3] Callus PJ, Mouritz AP, Bannister MK, Leong KH (1999) Tensile Properties and Failure Mechanisms of 3D Woven GRP Composites. *Compos Part A Appl Sci Manuf.* 30, 1277–87.
- [4] Brown D, Morgan M, McIlhagger R. A (2003), System for the Automatic Generation of Solid Models of Woven Structures. *Compos Part A Appl Sci Manuf.* 34, 511–5.
- [5] Sheng SZ, Hoa S V (2003), Modeling of 3D angle interlock woven fabric composites. *J Thermoplast Compos Mater.* 16, 45–58.
- [6] Cox BN, Dadkhah MS, Morris WL, Flintoff JG (1994), Failure Mechanisms of 3D Woven Composites in Tension, Compression and Bending. *Acta Matel Mater.* 42(12), 3967–84.
- [7] Thomson RS, Falzon PJ, Nicolaidis A, Leong KH, Ishikawa T (1999), The bending properties of integrally woven and unidirectional prepeg T-sections. *Compos Struct.* 47, 761–787
- [8] Chen X, Wang H (2006), Modelling and Computer-Aided Design of 3D Hollow Woven Reinforcement for Composites. *J Text Inst.* 97(1), 79–87.
- [9] Li Z, Sun B, Gu B (2010), FEM simulation of 3D angle-interlock woven composite under ballistic impact from unit cell approach. *Comput Mater Sci.* 49, 171-183
- [10] Shahkarami A, Vaziri R (2006), Acontinuum shell finite element model for impact simulation of woven fabric. *Int J Impact Eng.* 2006;1–16.
- [11] Tan P, Tong L, Steven GP (1998), Micromechanics models for mechanical and thermomechanical properties of 3D through the thickness angle interlock woven composites. *Compos Part A Appl Sci Manuf.* 30, 637–48.
- [12] Tsai KH, Chiu CH, Wu TH (2000), Fatigue behaviour of 3D multilayer-angle interlock woven composites plates. *Compos Sci Technol.* 60, 241–8.
- [13] Whitcomb J, Tang X (2001), Effective moduli of woven composites. *J Compos Mater.* 35(23), 2127–44.
- [14] Gu H, Gili Z (2002), Tensile Behaviour of 3D Woven Composites by Using Different Fabric Structures. *Mater Des.* 23, 671–4.
- [15] Adanur S, Liao T (1998), 3D Modeling of Textile Composite Preforms. *Compos Part B.* 29B, 787–93.
- [16] Hufenbach W, Hornig A, Gude M, Böhm R, Zahneisen F (2013), Influence of interface waviness on delamination characteristics and correlation of through-thickness tensile failure with mode I energy release rates in carbon fibre textile composites. *Mater Des* 50(0), 839–45.
- [17] Nasrun FMZ, Yahya MF, Ghani SA, Ahmad MR, Effect of weft density and yarn crimps towards tensile strength of 3D angle interlock woven fabric, *AIP Conference Proceedings* 1774, 020003(1-6), (2016), page. <https://doi.org/10.1063/1.4965051>
- [18] Dominy J, Rudd C (2002), Manufacturing with Thermosets. In: Long AC, editor. *Design and manufacture of textile composites.* Cambridge: Woodhead Publishing Limited, 181–96.
- [19] Chen X (2002), Mouldability of Angle Interlock for Technical Application. *Text Res J.* 72(3), 195–200.
- [20] Clark SR, Mouritz AP, Bannister MK (2003), Fibre Damage in the Manufacture of Advanced Three-Dimensional Woven Composites. *Compos Part A Appl Sci Manuf.* 34, 963–70.
- [21] Rudov-Clark S, Mouritz AP (2008), Tensile fatigue properties of a 3D orthogonal woven composite. *Compos Part A Appl Sci Manuf.* 39, 1018-1024
- [22] Talebi H, Wong S V, Hamouda AMS (2009), Finite element evaluation of projectile nose angle effects in ballistic perforation of high strength fabric. *Compos Struct.* 87, 314–20.
- [23] Tung PS, Jayaraman S (1991), Three-dimensional multilayer woven preforms for composites. In: Vigo TL, Turbak AF, editors. *School of Textile and Fiber Engineering.* Atlanta: Georgia Institute of Technology, 53–80.
- [24] Saleh MN, Yudhanto A, Potluri P, Lubineau G, Soutis C (2016), Characterising the loading direction sensitivity of 3D woven composites: Effect of z-binder architecture. *Compos Part A Appl Sci Manuf.* 90, 577–88.
- [25] Hamada H, Ramakrishna S, Huang ZM (1999), 3D Textile Reinforcement for Composites. First. Miravete A, editor. *Knitted fabric composites,* 181–91.